A proposal for performance evaluation of low frequency shielding efficiency

A proposal for performance evaluation of low frequency shielding efficiency

Aldo Canova[1], Luca Giaccone[1], Michele Quercio[1]*

[1]*Energy Department "G.Ferraris",Politecnico di Torino, Torino, Italy*
** aldo.canova@polito.it*

Keywords: Magnetic Shielding,Low Frequency,3D Magnetic Source

Abstract

The present work aims to propose a methodology for evaluating the performance of low-frequency magnetic shields used for the shielding of complex sources such as MV/LV substations. Today there is no standard procedure for testing shields based on the use of a single-coil for generating artificial MF(MF: Magnetic Field) as is the case for high-frequency anechoic chambers. In the case of shielding for industrial frequency sources, these are generally open shields with sources of various types: 3D transformers, switch-gear, and power lines. These kinds of sources and shields are better checked if the artificial MF has all three components in space. The work proposes a methodology based on the use of a tri-axial source, capable of generating a rotating magnetic field. The supports of the coils are made using a 3D printing process. The paper presents the design steps, the analytical performance evaluation of the source and the application to the test of a magnetic shield plate.

1 Introduction

The issue of evaluating the performance of shielding for electromagnetic fields at industrial frequency is currently an open problem. While there are guidelines for the characterization of shielding materials[1], nothing is defined for final shielding. A definition of some basic principles that guide a tester of a shielding system in his activity is therefore important and of great practical utility. In high frequency, some standards define how to measure the performance of a shielding room. The methodologies proposed by these standards are based on the use of two loops antennas, one source and one receiver, arranged in correspondence with two opposite faces of the shield [2,3]. The measurement can therefore be carried out at different points to verify the shielding efficiency of the entire shield. The validity of this procedure is based on the fact that the shield is of the closed type and the area to be protected is inside the shield. The situation is very different in the case of low-frequency magnetic fields. In this case, the shield is often placed close to the source and is very often of the open type. These two aspects lead us to think that performance evaluation must take into account aspects such as:

1. type of source: extension and position of the sources with respect to the shield.
2. geometry of the area to be protected: extension and position of the field points with respect to the source and the shield.

Correct testing can therefore only be carried out when the source has been completely installed and is sufficiently loaded (eg 25-30% of the rated load). On the contrary, to obviate the wait for the source to be put into operation, we often see tests in which, with the excuse of imitating what is proposed for radio frequencies, a field is generated with a small coil placed at a few tens of centimeters behind the screen and the magnetic field is measured with a probe placed a few centimeters on the other side of the screen. This type of test does not verify the shielding but gives us back the performance of the material as if the shield had infinite dimensions to the source. Therefore, if it is not possible to test the shielding by directly supplying the real source (eg panels, lines, and transformer of an MV / LV substation[4,5,6]) it would be advisable to simulate the sources through magnetic field generators placed at a sufficient distance from the screen, for example in the positions where the main components of the real source are located. In addition to this, a further approximation concerns the directionality of the magnetic field. In the case of a single-coil, the direction of the magnetic field is fixed in space and the module varies with a sinusoidal trend. In reality, magnetic fields have a three-dimensionality that changes over time, i.e. at a certain point, the magnetic field vector rotates in space. The three-dimensionality of the magnetic field must also be considered as the materials of the screens, depending on whether they are conductive or ferromagnetic, have different behavior depending on the angle of incidence of the magnetic field with the shielding surface. To simulate this phenomenon, it is, therefore, necessary to create a source capable of generating a rotating magnetic field. In the present work, we want to present a test methodology based on an artificial source capable of generating a rotating magnetic field. As an example, Fig.1 shows the artificial source made by a 3D printing process. The first comparisons between values calculated and measured on a single axis show an excellent response. The results obtained by feeding the source with three out of phase currents capable of generating a rotating field will be presented and the test methodology of a real shield will be presented.

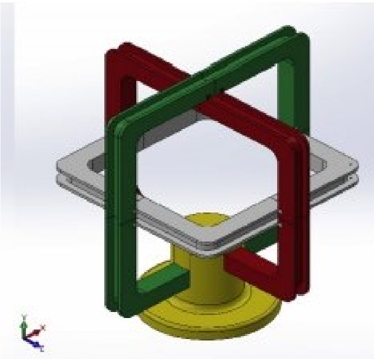

Fig. 1. 3D printing model of the artificial source

2 System description

The triaxial coil support system was designed in 3D through the use of Solidworks software and subsequently realized with a 3D printer. The sizing of the apparatus was carried out taking into consideration the magnetic field values to be generated. The procedure followed is illustrated below.

2.1 Numerical model of the magnetic field

The magnetic field generator is simulated by arranging the three coils in 3D space. Each coil was approximated with segments, which represent filiform conductors. The coils are wound along the perimeter of the support and are considered positioned side by side to the other in the available space. Figure 2 show this concept and the final result.

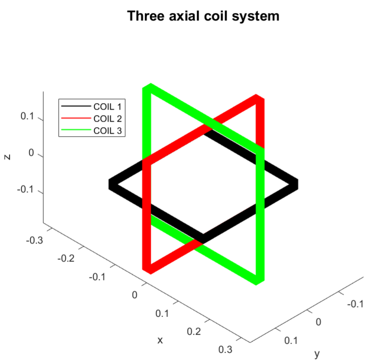

Fig. 2. Three axial coil simulation

The simulation of the magnetic field generated by the three coils was carried out using MATLAB software. The magnetic field was calculated for a single instant of time in a defined region of space and a series of field points. The waveforms of the three components of the magnetic field over time were analyzed, on a single field point. To identify the points of the magnetic field, a region has been defined centered on the origin of the axes (figure 3) and considering the center of the structure. The origin of the system is placed at the center of the three coils The magnetic induction **B** was calculated

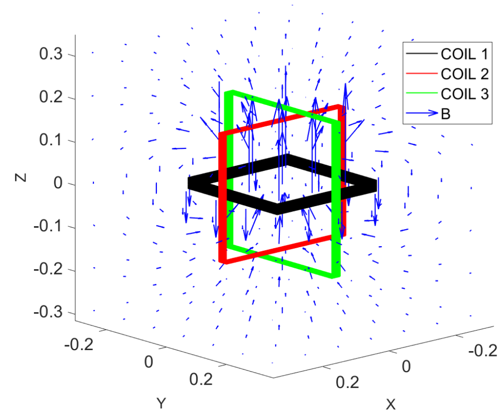

Fig. 3 Example of the magnetic induction trend calculated by powering the xy coil with unitary current.

through the superposition principle of the analytical closed form expression of the magnetic flux density produced by a straight segment(1)[6]. If P1, P2, are respectively the start point, the end point of the segment and P_Q is the field point, the formulation is:

$$\mathbf{B} = \int_{P_1}^{P_2} \frac{\mu_0 \times i}{4\pi} \times \frac{\mathbf{dl} \times \mathbf{r}}{r^3} \quad (1)$$

The function allows to calculate the magnetic field, generated by filiform conductors crossed by current i , in a series of points at a distance R. For evaluation in a single instant of time, the field is calculated considering the contributions of each coil individually. The total field is obtained through superposition theorem.

2.2 Coil sizing

The magnetic field strength is proportional to the number of turns of each coil and so, to maximize the field, it needs to maximize the product $N \times I_{max}$. The choice of the number of turns and the maximum current is based on the consideration of some power constraints. The supply system is based on a signal generator that controls a power amplifier. This allows to generate an arbitrary waveform or to control the frequency of a sinusoidal current in a range from some hertz to some kilohertz. Each coil is a load of each channel of the power amplifier and to exploit the maximum power the coil impedance should be adapted to a value of 2 or 4 ohm. For this reason, is important to preliminary evaluate the inductance of each coil. The evaluation of the impedance Z has been calculated for each of the three rectangular rings because they have different dimensions.

Then the inductance L was calculated for each loop, using the formula:

$$L_s = \frac{\mu_0}{\pi} \times [-2 \times (W+H) + 2 \times \sqrt{(H^2+W^2)} - H \times ln\frac{H+\sqrt{(H^2+W^2)}}{W} - W \times ln\frac{(W+\sqrt{(H^2+W^2)}}{H}) + H \times ln\frac{2 \times H}{\frac{d}{2}} + W \times ln\frac{2 \times W}{\frac{d}{2}}$$

Where:

- W is the longitudinal dimension of the coil.
- H is the transversal dimension of the coil.
- μ_0 is the permeability magnetic vacuum.
- d is the cable diameter(or equivalent one in the case of rectangular cross section)

3 Experimental activity

3.1 Measurements

In a first test analysis three groups of measures have been created, alternately feeding coil 1(white), coil 2 (red) and finally both simultaneously.

- Coil 1

The measurements were made in three different points of the structure (figure 4). The acquisitions have been made with the oscilloscope on an electrical period. Coil 1 was powered with a current equal to:

$$I = \sqrt{2} \times 0.5 \times sin(\omega t) \text{ f=45 Hz}$$

Fig. 4. Some typical points of measurement

- Coil 2

The procedure is the same as the previous one. The frequency of 45 Hz was chosen in order to avoid the disturbances at 50 Hz. The value of the current in the coil 2 was:

$$I = \sqrt{2} \times 0.9 \times sin(\omega t) \text{ f=45 Hz}$$

In this case, the expected main induction direction is along the x-axis. Considering however the transformation into global coordinates, the measurement results are more affected by a coordinate error. In particular, the measure doesn't show a relevant component in the z-axis. The presence of the component in the z-axis is justifiable by the curvature that the field lines undergo to that distance from the structure since they tend to close.

- Coil 1 and Coil 2

The measurements were carried out at the center of the structure and externally, in order to evaluate the different intensity of the generated field.

$$I1 = \sqrt{2} \times 0.5 \times sin(\omega t) \; I2 = \sqrt{2} \times 0.9 \times sin(\omega t) \text{ f=45 Hz}$$

Test 8 was carried out in the center of the structure with two equal-sized currents, offset by 60°

$$I1 = \sqrt{2} \times 0.9 \times sin(\omega t) \; I2 = \sqrt{2} \times 0.9 \times sin(\omega t) \text{ f=45 Hz}$$

3.2 Numerical and experimental comparison

A comparison between the experimental measurements and the results of Matlab simulations had been made considering the RMS value of the waveforms resulting from magnetic induction. In Fig. 5 are indicated the values of the three magnetic induction components, both for the experimental measurements and for Matlab simulations. The overall RMS was obtained with the vector sum of the three components:

$$B_{rms} = \sqrt{(Bx^2 + By^2 + Bz^2)}$$

TEST	I1 RMS	I2 RMS	EXPERIMENTAL RESULTS				SIMULATIONS RESULTS				ε %
			Bx MEAS	By MEAS	Bz MEAS	BRMS MEAS	Bx SIM	BY SIM	Bz SIM	BRMS SIM	
	[A]	[A]	[μT]	[μT]	[μT]	[μT]	[μT]	[μT]	[μT]	[μT]	[%]
1	0.5	-	30.7	9.19	48.1	57.8	0	0	57.9	57.9	0.3
2	0.5	-	75.2	25.9	215.4	229.6	0	0	225	225	2.1
3	0.5	-	60.4	154.9	361	397.5	58	58	396	404.4	1.7
4	-	0.9	187.4	19.6	21.5	189.7	185	0	15.3	185.6	2.2
5	-	0.9	386.7	22.3	29.2	388.4	364.2	0	0	364.2	6.7
6	-	0.9	35.5	2.7	3.9	35.8	31.6	0	17.2	35.9	0.5
7	0.5	0.9	34.9	4.6	12.9	37.5	30.3	0	20	36.3	3.3
8	0.9	0.9	294.4	52.1	335	449.01	332.1	0	362.8	491.4	8.7

Fig. 5. Data results

It is observed that the intensity of the field outside the structure is lower than inside with values that are between 50 μT for field points close to the coils (test 1) and 35 μT for field points spaced 20 cm from the structure (tests 6-7). Comparing the measurements made at the central point of the structure (tests 2, 5, 8) it is evident that the value of induction in test 8 is greater than test 2 and test 5. This happens because two coils are fed, and the overall magnetic induction is obtained from the superposition of individual effects. The sum of the contribution of coil 1 and coil 2 fed at the same time it is not the same as the contribution of the individual coils fed individually, because part of the effect of one coil is compensated by the effect of the other: consequently test 8 has a value not much greater than in test 5, even though both coils are powered with 0.9 A RMS. To characterize the device, further measures were carried out for completeness. In particular, the maximum distance at which the device provides an acceptable magnetic field value was evaluated. The simulation results reflect the real ones Fig.6

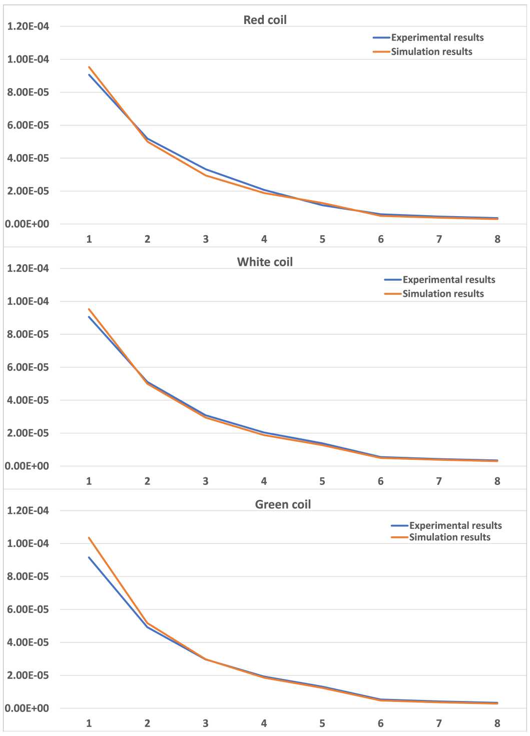

Fig. 6. Comparison simulation-real results

4 Methodology for the testing of a shield plate

The set-up for the testing of a magnetic field shield is schematized in Fig.7 and show in Fig.8

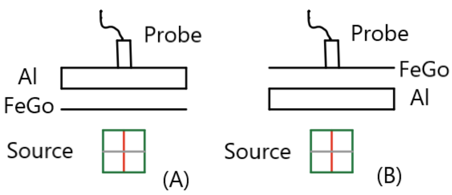

Fig. 7. Set-up configurations

The goal of this test is to characterize a shield sample under a magnetic field with different vector components. The shield samples under test have a multi-layer structure based on conductive and ferromagnetic material Al and FeGo respectively: aluminum (Al) and grain-oriented silicon iron(FeGo)[7,8]. Two different plate configurations have been analyzed with two different aluminum thicknesses(2,7 and 4 mm) and the same number of FeGo sheets (2). The procedure consists of a first

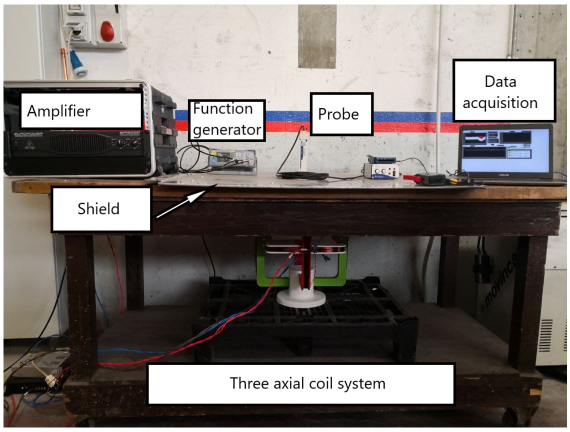

Fig. 8. Test shielding system

step in which one coil at a time is powered and the magnetic field values are measured with and without the shield. To evaluate the shielding coefficient for each axis component. Table 1 highlights the supply coils configurations.

Table 1 Supply coil configurations

Test case	Prevalent component	Coil fed
1	Z	White
2	Y	Red
3	X	Green
4-5	Y-Z	Red-White
6-7	X-Y	Green-Red
8-9	X-Z	Green-White
10-11-12	X-Y-Z	Green-Red-White

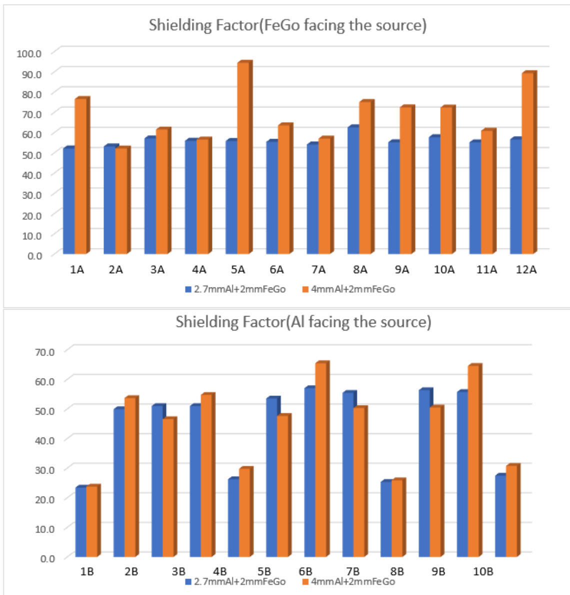

Fig. 9. SF results

In Fig.8 are reported the two set-up configurations regarding the orientation of the shield concerning the source and the probe. Conf.A put the Al to the side of the probe and the FeGo to the side of the source; Conf. B is the opposite. The results obtained for the two configurations in terms of shielding factor (SF= ratio between the magnetic induction component with and without the shield) are reported in Fig.9. Some general conclusion can be done:

- The aluminum thickness increase significantly the SF in conf. A and when the MF has a z-component (component normal to the shield)
- In conf. A the plate with higher Al thickness has always better performances, this is not true for conf. B
- Conf. A and B have similar SF values (between 50 and 65); The only configurations that show very different performances are those when z component is present(1-5-9-12).

5 Conclusion

In this paper, an innovative MF source for the testing of low-frequency magnetic shielding is presented. The proposed source is composed of three coils for the generation of rotational MF in space. The presence of all the axial components of the magnetic field allows to better test magnetic shield performances independent from the shield material: conductive, ferromagnetic, or mixed. The source has been applied during the test procedure of a sample plate but it can applied also during the test of a real shield.

6 Acknowledgment

We want to thank the BEShielding SRL company (WWW.BESHIELDING.IT) for providing the sample of material on which the tests were carried out.

7 References

[1] ASTM A698 / A698M – 20 Standard Test Method for Magnetic Shield Efficiency in Attenuating Alternating Magnetic Fields
[2] EN 50147-1 Anechoic chambers – Part 1: shield attenuation measurements
[3] IEC 61000-4-8: ‘Electromagnetic compatibility (EMC) – Part 4–8: testing and measurement techniques – power frequency magnetic field immunity test’, 2009
[4] Juan Carlos del-Pino-López et al."Design of active loops for magnetic field mitigation in MV/LV substation surroundings",Electric Power Systems Research Volume 119, February 2015, Pages 337-344
[5] Mitigation techniques of power frequency magnetic fields originated from electric power systems, Tech. Rep. Working group C4.204, CIGRE’, 2009
[6] Canova et al. "Description of Power Lines By Equivalent Source System",COMPEL Vol. 24, No. 3, 2005, pp. 893-905
[7] Bavastro, D.et al.: ‘Numerical and experimental development of multilayer magnetic shields’, Electric Power Syst. Res., 2014, 116, pp. 374–380
[8] Canova A.,"Multilayer magnetic shielding: an innovative overlapping structure", October 2017CIRED - Open Access Proceedings Journal 2017(1):780-783; DOI: 10.1049/oap-cired.2017.0487